CHAPTER 104

FORCES ON AND PARTICLE MOTIONS AROUND SUBMERGED STRUCTURES IN STEEP WAVES

JESPER SKOUROUP [1] and IVAR G. JONSSON [2]

Abstract

A boundary integral equation method combined with a non-linear time stepping procedure for the free water surface is developed for simulations of the interaction between highly non-linear water waves and fixed submerged horizontal cylinders.

The wave forces on the cylinders are computed and a good correspondence is found with other computed results for low Keulegan-Carpenter numbers.

A new method for tracing the orbits of water particles in the fluid domain is developed, and the influence from submerged structures on the orbits is visualized through some computational examples.

Introduction

The numerical modelling of the interaction between highly non-linear water waves and large structures has been a field of growing interest during the last decade. These studies are motivated by the desire to obtain a numerical model in which simulations of wave/structure interactions can be performed, and hence establish an alternative to physical model tests. Among the numerical models based on a potential theory formulation the Boundary Integral Equation Method (BIEM) turns out to be one of the most efficient ones.

The first contribution where the BIEM was used for the modelling of steep and overturning waves was given by Longuet-Higgins & Cokelet (1976). They used a formulation based on Green's 2nd identity, but in a conformably map-

---

1)Danish Hydraulic Institute, DK-2970 Hørsholm, Denmark.
2)Institute of Hydrodynamics and Hydraulic Engineering (ISVA), Technical University of Denmark, DK-2800 Lyngby. DENMARK

ped space, and the computations were thus restricted to two spatial dimensions (2-D).

Use of a BIEM based on the Cauchy integral theorem was made by Brevig et al. (1981), and they computed the wave forces on a submerged horizontal circular cylinder (pipeline) caused by breaking waves.

Stansby and Slaouti (1984) also used a formulation based on the Cauchy integral theorem in their computations of wave forces on a horizontal circular cylinder, and they obtained results which were in good agreement with the analytic results of Ogilvie (1963).

An efficient method for the temporal updating of the free water surface was developed by Dold & Peregrine (1984). In this method the influence of the higher order derivatives along the free water surface was taken into account, and this permitted the use of large time-steps with a good accuracy, and the method became very efficient for the modelling of e.g. overturning waves. In their model a conformably mapped space and Cauchy's integral theorem were used, and hence their computations (as in the previous models) were restricted to 2-D problems.

In the present paper a 2-D physical-space, non-linear BIEM is used for the modelling of steep water waves and for wave-structure interactions, and contrary to the 2-D models described above, there are in principle no restrictions for this model to be extended to 3-D.

A simple method (based on the BIEM) for a time-stepping of water particles within the fluid domain is developed and used for tracing particle orbits in time. Fixed structures are incorporated into the model, and the flow field around them are evaluated by use of the time-stepping of interior points.

Furthermore the wave forces on the structures are computed, and the "shielding" and "blockage" effects are shown for the case of two parallel cylinders.

Mathematical Formulation

The irrotational flow of an incompressible fluid with a free surface is considered. Within the frame of potential theory the flow can be described by a velocity potential $\phi(\mathbf{x},t)$, and the fluid velocity is then given by $\mathbf{u} = (u,w) = (\phi_x,\phi_z) = \nabla\phi$ where $\mathbf{x} = (x,z)$ is a position vector of an "observation point" and t is the time. By use of the mass conservation equation in the fluid domain $\Omega(t)$ (depicted in Fig. 1) we find that ϕ satisfies the Laplace equation throughout the fluid domain, i.e.

$$\nabla^2\phi = 0. \tag{1}$$

The boundary conditions for ϕ on the free surface $\Gamma_f(t)$ are the kinematic condition

$$\frac{D\vec{r}}{Dt} = (\frac{\partial}{\partial t} + \vec{u}\cdot\nabla)\vec{r} = \vec{u} = \nabla\phi, \quad z = \eta \tag{2}$$

where $\vec{r}$ is a position vector of a water particle at the free surface, and the dynamic condition (Bernoulli's equation)

$$\frac{D\phi}{Dt} = - gz + \frac{1}{2}|\nabla\phi|^2 - \frac{p_a}{\rho}, \quad z = \eta \tag{3}$$

($D\phi/Dt = \phi_t + |\nabla\phi|^2$ is a particle following (Lagrangian) operator, and ϕ_t is an abbreviation of $\partial\phi/\partial t$). In (3), g is the acceleration due to gravity, p_a is the atmospheric pressure, and ρ is the density of water (here taken as 10^3 kg/m³).

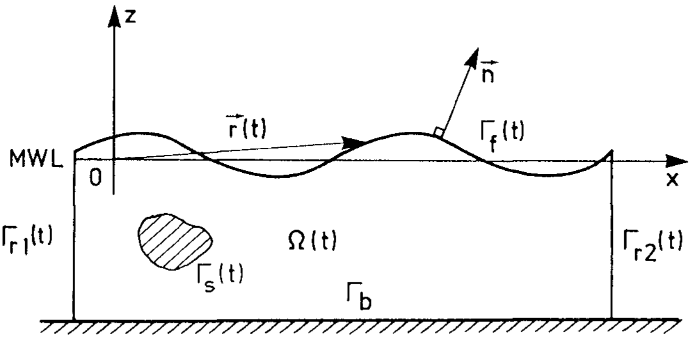

Fig. 1 Calculation domain and definition of boundaries. The x-axis is at the mean water level (MWL).

On the stationary bottom Γ_b (which is horizontal and impermeable) the boundary condition is

$$\phi_n = 0 \quad , \ z = -h \tag{4}$$

where n is the coordinate along the unit normal vector $\vec{n}$ pointing outwards from the fluid domain (and ϕ_n is an abbreviation of $\partial\phi/\partial n$).

When a structure is situated in the computational domain, the boundary condition on its surface $\Gamma_s(t)$ is

$$\phi_n = \nabla\phi\cdot\vec{n} = V_s \tag{5}$$

where V_s is a function describing the velocity of the body surface in the direction of the unit normal vector $\vec{n}$. In the case of a fixed structure $V_s = 0$.

Boundary conditions at the lateral boundaries $\Gamma_{r1}(t)$ and $\Gamma_{r2}(t)$ are needed for a closure of the boundary value problem for ϕ. By assuming space periodicity (but not necessarily time periodicity) and no net current below wave trough level, periodicity conditions can be imposed on the vertical boundaries $\Gamma_{r1}(t)$ and $\Gamma_{r2}(t)$

$$\phi_n\left[\Gamma_{r1}(t)\right] = -\phi_n\left[\Gamma_{r2}(t)\right], \quad \phi\left[\Gamma_{r2}(t)\right] = \phi\left[\Gamma_{r1}(t)\right] \tag{6}$$

for the same z-values at the two boundaries. The horizontal distance between $\Gamma_{r1}(t)$ and $\Gamma_{r2}(t)$ has to be an integer number of wave lengths. Periodicity conditions at the lateral boundaries were also used by Brevig et al. (1981) and by Stansby and Slaouti (1984) in their studies of wave/structure interaction by use of the BIEM.

In order to solve the Laplace problem (1) with the fully non-linear boundary conditions we use an integral equation method based on Green's 2nd identity

$$\alpha(\vec{x})\phi(\vec{x},t) = \int_{\Gamma(t)} \phi(\vec{\xi},t)G_n(\vec{x},\vec{\xi}) - G(\vec{x},\vec{\xi})\phi_n(\vec{\xi},t)\, d\Gamma \tag{7}$$

where $\vec{\xi}$ is the position vector of an "integration point" situated at the boundary $\Gamma(t)$.

The kernel function $G(\vec{x},\vec{\xi})$ is the free space Green's function which in two dimensions is:

$$G(\vec{x},\vec{\xi}) = \ln|\vec{\xi}-\vec{x}| \tag{8}$$

The factor $\alpha(\vec{x})$ depends on the boundary geometry ($\alpha(\vec{x}) = \pi$ for $\vec{x}$ at a smooth part of the boundary, and $\alpha(\vec{x}) = 2\pi$ for $\vec{x}$ inside $\Omega(t)$).

The derivative of G in the direction of the outwards unit normal vector $\vec{n}$ is

$$G_n(\vec{x},\vec{\xi}) = \frac{(\vec{\xi}-\vec{x})\cdot\vec{n}}{|\vec{\xi}-\vec{x}|^2} \tag{9}$$

Following the solution of the Laplace problem for ϕ an updating in time of the computational domain and related boundary conditions to a subsequent time level must be performed. Using the Lagrangian approach developed by Dold & Peregrine (1984), truncated Taylor series in time for the position vector $\vec{r}$ of a free surface particle and for the velocity potential ϕ provide

$$\vec{r}(t+\Delta t) = \vec{r}(t) + \sum_{k=1}^{n} \frac{(\Delta t)^k}{k!}\frac{D^k\vec{r}(t)}{Dt^k} + O[(\Delta t)^{n+1}] \tag{10}$$

$$\phi(\vec{r}(t+\Delta t),t+\Delta t) = \phi(\vec{r}(t),t) + \sum_{k=1}^{n} \frac{(\Delta t)^k}{k!}\frac{D^k\phi(\vec{r}(t),t)}{Dt^k} + O[(\Delta t)^{n+1}] \tag{11}$$

where Δt is the time increment, and the Lagrangian (particle following) operator D/Dt is defined in (2).

The expansion coefficients in (10) and (11) are obtained by successive solutions of the Laplace equation for the velocity potential ϕ and its time derivatives, where the solution of one Laplace problem provides the non-linear boundary conditions for the next.

The solution of the Laplace problem for ϕ by use of Green's 2nd identity (7) gives as result ϕ and ϕ_n at the whole boundary of the computational domain. Hence the gradient of the velocity potential can be evaluated, and thereby the first order expansion coefficients in (10) and (11) by use of the free surface boundary conditions (2) and (3).

The boundary condition at the free surface for the Laplace problem involving the first order time derivative is obtained from the Eulerian form of the dynamic condition at the free surface (cf. (3)).

$$\phi_t = - gz - \frac{1}{2}|\nabla\phi|^2 - \frac{p_a}{\rho}, \qquad z = \eta \tag{12}$$

The conditions at the remaining part of the boundary are obtained by differentiating (4), (5), and (6) with respect to t.

Just as the governing differential equation (1) and the integral equation (7) are valid for ϕ, these may also be written for time derivatives of any order of ϕ. Hence we have a mathematical problem formulated in the same geometry as before, but now with ϕ_t and ϕ_{tn} as solution at the boundary of the computational domain. The numerical solution of the second (and of subsequent) Laplace problems is computationally very fast compared to the solution of the first Laplace problem since the kernel functions (G, G_n) of the governing integral equation only are functions of the boundary geometry which is unchanged, since all derivatives are computed at the same time level. In the present work the series (10) and (11) are truncated after n=2, but it is mentioned that the expansion coefficients are obtained from the fully non-linear boundary conditions at the free surface.

The lateral boundaries of the computational domain are updated by following the horizontal motion of the intersections with the free surface.

After the solutions of the Laplace problems for ϕ and ϕ_t have been found by use of the BIEM, all variables of interest at the boundary of the computational domain are determined. By use of (7) it is thus possible to determine the values of the velocity potential ϕ and its time derivative ϕ_t at any point <u>inside</u> the computational domain $\Omega(t)$. Furthermore, analytical differentiations of (7) provide integral equations to determine the values of ϕ_x, ϕ_z, ϕ_{xt}, ϕ_{zt}, ϕ_{xx} and ϕ_{xz} at the observation point $\vec{x}$.

These functions only appear as unknowns outside the relevant integrals (since G and its derivatives are functions of the geometry, which is known), and the numerical evaluation of them is therefore very fast. From the results we may deduce the particle velocity components u and w, the acceleration components a_x and a_z, and the dynamic pressure p^+ (= p + ρgz) at the interior point given by the position vector x as:

$$u(\vec{x}) = \phi_x(\vec{x}) \tag{13}$$

$$w(\vec{x}) = \phi_z(\vec{x}) \tag{14}$$

$$a_x(\vec{x}) = \phi_{xt}(\vec{x}) + \phi_{xx}(\vec{x})\phi_x(\vec{x}) + \phi_{xz}(\vec{x})\phi_z(\vec{x}) \tag{15}$$

$$a_z(\vec{x}) = \phi_{zt}(\vec{x}) + \phi_{xz}(\vec{x})\phi_x(\vec{x}) - \phi_{xx}(\vec{x})\phi_z(\vec{x}) \tag{16}$$

$$p^+(\vec{x}) = -\rho[\phi_t(\vec{x}) + \frac{1}{2}\{(\phi_x(\vec{x}))^2 + (\phi_z(\vec{x}))^2\}] \tag{17}$$

where in (16) $\phi_{zz}(\vec{x})$ has been replaced by $-\phi_{xx}(\vec{x})$.

A time-stepping method for water particles in the fluid domain $\Omega(t)$ similar to the one for updating of particles at the free water surface (i.e. based on truncated Taylor series) may then be written as:

$$x_i(t+\Delta t) = x_i(t) + u(\vec{x})\Delta t + a_x(\vec{x}) \frac{(\Delta t)^2}{2} + O[(\Delta t)^3] \tag{18}$$

$$z_i(t+\Delta t) = z_i(t) + w(\vec{x})\Delta t + a_z(\vec{x}) \frac{(\Delta t)^2}{2} + O[(\Delta t)^3] \tag{19}$$

where the position vector of the water particle is $\vec{x}$ = (x_i, z_i). Hence we have established a visualization technique that enables us to follow the traces of water particles in the fluid domain in time.

Numerical Solution Method

The boundary of the computational domain is subdivided into a finite number of small segments, each segment connecting two adjacent discretization points situated at the boundary curve. By representing the geometry as well as the boundary functions ϕ and ϕ_n at each segment by a prescribed variation, the governing integral equation can be formulated in terms of the values of the variables ϕ and ϕ_n (or ϕ_t and ϕ_{tn}) in the discretization points. Hence we may form a linear algebraic system of equations, in which each element only is a function of the geometry of the boundary and of the interpolation functions used.

In order to model the variation of boundary functions between the discretization points, we use a Hermite cubic spline representation along each boundary element at the free surface (i.e. between two adjacent discretization points) and a linear variation elsewhere. By this method a continuity up to and including 2nd order derivatives of the free surface representation is kept, and all boundary nodes there are treated equally in the numerical solution of the governing integral equation.

The numerical integration over each regular boundary element (i.e. an element where the integration point does not coincide with the observation point) is performed by use of a standard Gauss-Legendre quadrature. At the singular boundary elements special methods must be used (see Skourup (1989) for details).

Results

During recent years, particular attention has been paid to numerical simulations of the interaction between waves and submerged floating structures with large dimensions. Especially a new concept for crossing of deep fjords and straits with submerged tunnels (which e.g. has been proposed for a strait crossing at Högsfjord, Norway) has inspired to the work presented in this paper.

In all the following computations the Keulegan-Carpenter number K is smaller than 2 and the predominant contribution to the force on the structure is thus inertial and can be computed by the BIEM.

The total wave force vector $\vec{F}$ on the structure, which is cylindrical, is obtained by integrating the excess pressure p^+ (due to the waves) over the whole surface of the structure.

$$\vec{F} = - \int_{\Gamma_s} p^+ \vec{n} \, d\Gamma \tag{20}$$

where $\vec{n}$ is the outward normal unit vector from the surface of the cylinder. The excess pressure p^+ is determined from the Bernoulli equation as

$$p^+ = - \rho [\phi_t + \tfrac{1}{2}(\phi_s{}^2 + \phi_n{}^2)] \tag{21}$$

where ϕ_n vanishes at the surface of the cylinder (since it is fixed and impermeable). The term ϕ_s is found from the spatial derivatives of ϕ at Γ_s.

One Circular Cylinder

The special reference case with computation of the interaction between waves and a submerged horizontal circular cylinder with its axis parallel to the wave crests has been treated widely in the literature, beginning with Dean (1948), who showed that linear deep water waves undergo a phase shift as they pass over a cylinder, and further that there is no reflection from the cylinder. Ursell (1950) used a multipole method, and derived expressions for the first-order forces on the cylinder. Ogilvie (1963) extended Ursell's method and provided expressions for the mean second order ("drift") force at the cylinder. Chaplin (1984a,b) performed experiments to determine the non-linear forces and mass transport around a horizontal submerged cylinder, and experimentally verified that there is a mass-transport around the cylinder, as it could be predicted by use of Milne-Thomson's (1968) circle theorem.

A fluid domain with a horizontal dimension of one wave length L is considered. In this domain we situate a fixed horizontal circular cylinder with diameter D = 2a (a being the radius of the cylinder) and a submergence d of its centre axis as depicted in Fig. 2.

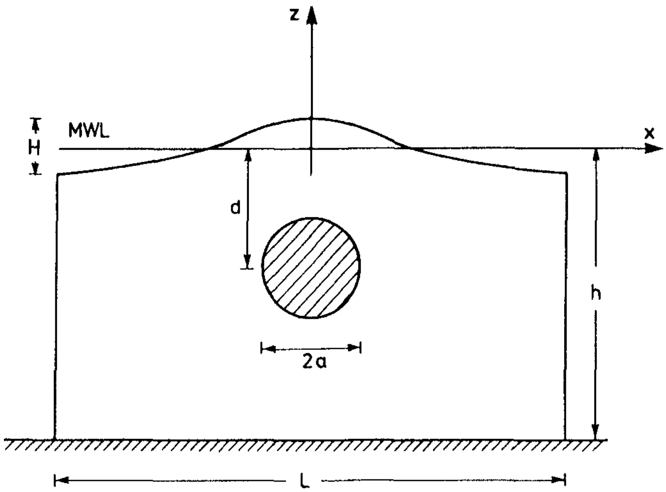

Fig. 2 Definition sketch of submergence d and radius a of horizontal circular cylinder.

The diameter of the cylinder is D = 10.0 m and the submergence is d = 20.0 m. The wave data are: H = 10.0 m, T = 8.78 s, at a depth h = 100 m and an initial profile given by the stream function wave theory by Rienecker & Fenton (1981). This gives a wave length L = 128 m and hence a steepness of the wave of 7.8%, and the Keulegan-Carpenter number K = 1.2. Computations are carried out covering 6 wave periods with time steps of T/100, and the resulting wave force variation in time on the cylinder is depicted in Fig. 3. The total force on the cylinder is computed as the modulus of the two force components F_x and F_z.

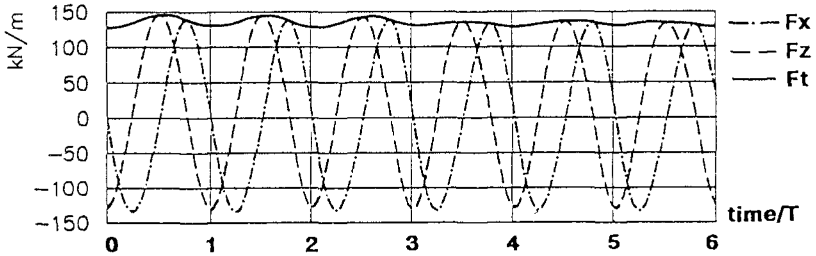

Fig. 3 Wave force on a horizontal cylinder during 6 wave periods. Domain length is L.

By regarding Fig. 3 it is readily seen that the oscillations of the total force tend to decrease as the computations proceed in time. In order to investigate if this is an effect arising from using the periodicity conditions at the lateral boundaries with a distance of just one wave length, the same computation is carried out with identical wave and structure data, but now with the horizontal dimension of the computational domain of either three or five wave lengths (i.e. the spacing of the cylinders is either 3L or 5L).

In Fig. 4 the total force on the cylinder is compared for the horizontal dimension of the computational domain being either one or three wave lengths.

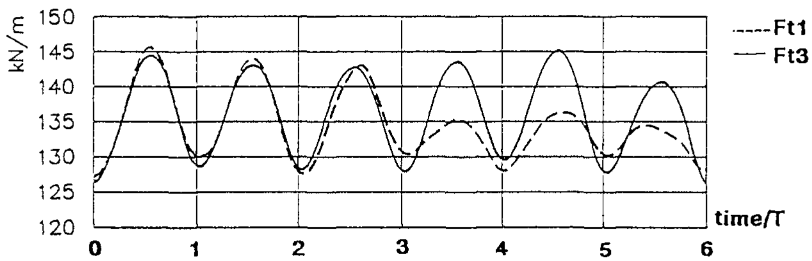

Fig. 4 Total wave forces on a cylinder during 6 wave periods. Domain length is either L or 3L.

During the first three wave periods the difference between the two results is less than 1.5% of the mean total force on the cylinder. The larger deviation hereafter is probably an effect of the proximity of other cylinders. Extending the horizontal dimension of the computational domain further to five wave lengths provides almost identical results as obtained from the domain, which was three wave lengths long, when the first three wave periods are considered.

From these computational results we conclude that a horizontal dimension of one wave length is sufficient for computations covering a time span less than three wave periods. It is mentioned that the computational time is proportional to N^3 for large values of N (where N is the number of computational nodes at the boundary), and the desired accuracy of the results therefore must be assessed against the computational time necessary to provide the results.

Numerical results for the interaction between nonlinear waves and a submerged horizontal, circular cylinder at low Keulegan-Carpenter numbers, are found in Stansby & Slaouti (1984), in Vada (1987), and in Isaacson & Cheung (1990), and in all cases the inertia coefficients are in the same range as the present results.

Experimental results are also available, and for deeply submerged cylinders Cheong et al. (1989) found the inertia coefficients to be in the vicinity of 2 for low Keulegan-Carpenter numbers. For a cylinder close to the free surface, Chaplin (1984b) and Miyata & Lee (1990) found the inertia coefficients to be much smaller than 2 in their experiments with Keulegan-Carpenter numbers in the range 1-3. Chaplin (1984b) explained this decrease as associated with the circulation generated by steady streaming in the oscillatory boundary layer on the cylinder. It has not been possible in the present work to reproduce these low inertia coefficients. This indicates that the large reduction of the inertia coefficients is an effect due to viscosity, which is omitted in the present work. Miyata & Lee (1990) obtained this large decrease of the inertia coefficient in their computations where they solved the Navier-Stokes equations in a finite difference formulation for Reynolds numbers $1.69 \cdot 10^4$ and $3.87 \cdot 10^4$.

Tracing of the orbits of water particles in the vicinity of the cylinder is performed by use of the time stepping method for particles in the fluid domain (i.e. eqs. (18) and (19)).

In Fig. 5 the particle motion during one (Eulerian) wave period is followed. It is seen that the water particles tend to follow the cylinder contour and that they have all moved to new positions in the clockwise direction around the cylinder after one wave period. This circulation of water particles around a horizontal cylinder is also showed analytically by e.g. Ogilvie (1963), and verified experimentally by Chaplin (1984a). The amplitudes (both in the horizontal and the vertical directions) are by linear wave theory found to be 2.77 m for a water particle at z = -12.0 m, and this corresponds quite well with the orbits shown in Fig. 5.

Particle orbits in the vicinity of the cylinder are also computed using the circle theorem (cf. Milne-Thomson, 1968) combined with a time-stepping procedure (as (18) and (19)) for water particles and good agreement was found with orbits computed by the BIEM.

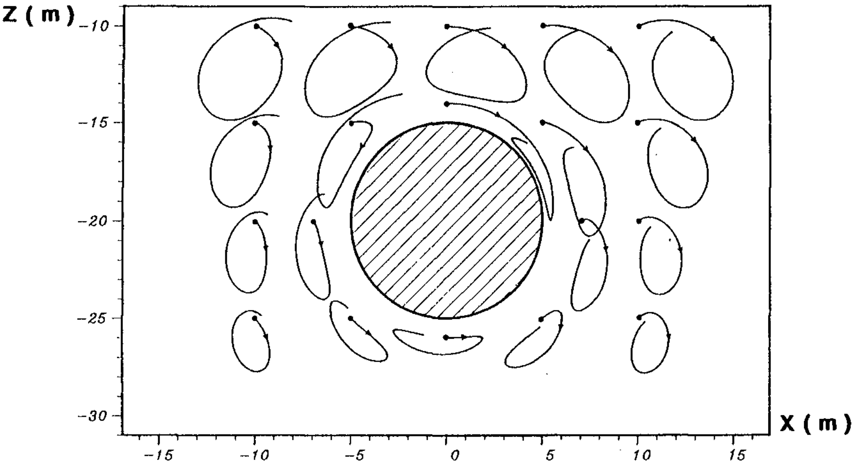

Fig. 5 Traces of the particle motions during one period in the vicinity of a submerged, circular cylinder with diameter D = 10.0 m. Wave data: T = 8.78 s, H = 10.0 m, L = 128 m at h = 100 m. ●: initial position, ►: orbital direction. Domain length L.

Two Circular Cylinders

Computations with more than one cylinder in the fluid domain are also performed.

Two parallel horizontal circular cylinders are considered, and the dimensions of the cylinders are kept the same as in the previous case, i.e. with a diameter D=10.0m, and a submergence of their centre lines at d=20.0m. The wave data are also the same as before. The length of the computational domain equals L. In order to investigate the shielding and blockage effects between the two cylinders, computations with different distances between the centre lines have been carried out covering three wave periods. The distances have been chosen as 1.5D, 2D and 3D and the main results are given in Table I. Here also the reference-numbers corresponding to an "infinite" distance between the cylinders are given. These reference numbers are computed during the second and third wave period for the case with one cylinder in a domain with length 5L.

From Table I two different effects from the interaction between the two cylinders appear. Regarding the horizontal force F_x on each of the two cylinders it is seen that the amplitudes are decreasing as the cylinders are approached to each other, and that the force amplitude is larger on the upstream cylinder than on the downstream cylinder. This is due to a shielding effect between the two cylinders.

Cylinder	Centre axis dist.	$F_{x,max}$	$F_{x,min}$	$F_{z,max}$	$F_{z,min}$	$F_{t,max}$	$F_{t,min}$
1	1.5D	138.1	-123.2	160.3	-142.9	162.0	116.4
(upstream)	2D	139.9	-129.5	151.6	-134.1	154.5	122.3
	3D	142.4	-134.0	145.4	-128.4	149.1	122.8
2	1.5D	126.1	-122.7	155.0	-146.4	155.6	116.9
(downstream)	2D	131.7	-125.6	145.0	-137.5	146.5	119.9
	3D	134.4	-130.4	138.7	-132.8	141.3	121.7
	"∞"	137.6	-134.2	142.9	-128.4	143.0	128.1

Table I Extreme wave force amplitudes (in kN/m) at two parallel cylinders as function of centre axes distance. The computations cover 3 wave periods.

Regarding the vertical force F_z on each of the two cylinders it is seen that the amplitudes are increasing as they are approached to each other. This result shows that there is a blockage effect between the two cylinders. The maximum force amplitude is slightly larger on the upstream cylinder than on the downstream cylinder.

The sum of the shielding and the blockage effects between the two cylinders appear in the total force variation at the two cylinders, and it is seen that the effect from blockage influences the total force, since the maximum values of the total force on each of the two cylinders increase as the they are approached to each other.

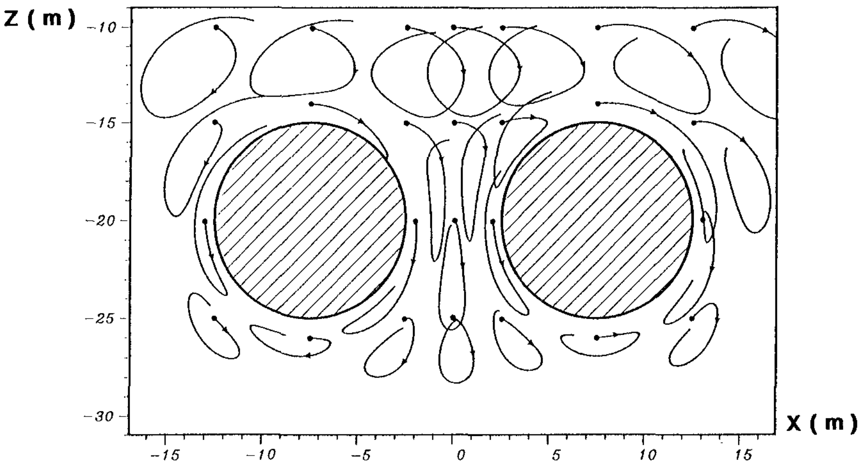

Fig. 6 Particle orbits in the vicinity of two parallel horizontal circular cylinders with centre axis distance 1.5D. Other data as in Fig. 5.

The shielding effect between the two cylinders is seen only to have a small influence on the maximum value of the total force on the two cylinders.

Particle orbits in the vicinity of the cylinders are shown in Fig. 6 for a centre axis distance 1.5D.

Conclusion

It has been demonstrated that a fully non-linear boundary element model with periodicity conditions at the lateral boundaries of the computational domain provides good results for wave forces on and particle orbits around submerged horizontal cylindrical structures (2-D) for small Keulegan-Carpenter numbers. The effects from shielding and blockage between two cylinders are shown by computational examples, and the cylinder distances are found to have some effect on the forces.

There are, in principle, no restrictions in the mathematical formulation that prevent the present model from being extended to 3-D. However, appropriate conditions at the lateral boundaries of the computational domain must be developed in order to be able to perform computations with 3-D waves of not permanent form. Furthermore, faster and more efficient computers than those of today must be developed before an accurate non-linear 3-D model can be developed and used for application as a "numerical wave tank".

A more detailed account of the present study will be published subsequently (Skourup & Jonsson, 1990).

Acknowledgement

Most of the work presented in this paper was done as part of the first author's Ph.D. studies at ISVA at the Technical University of Denmark under the supervision of Assoc. Professor Ib A. Svendsen and later under the supervision of Assoc. Professor Ivar G. Jonsson. Jesper Larsen, Ph.D., acted as co-supervisor.

A large part of the work was performed at the University of Delaware, U.S.A., in close collaboration with Stephan T. Grilli, Ph.D., and Professor Ib. A. Svendsen.

The Danish Technical Research Council (STVF) has financed the present study (J. No. 5.17.3.6.03). This support is gratefully acknowledged.

References

Brevig, P., Greenhow, M. and Vinje, T. (1981). Extreme wave forces on submerged cylinders. 2nd Int. Symp. on Wave and Tidal Energy. Cambridge, England, Paper E2, 143-166.

Chaplin, J.R. (1984a). Mass transport around a horizontal cylinder beneath waves. J. Fluid Mech. 140, 175-187.

Chaplin, J.R. (1984b).Non-linear forces on a horizontal cylinder beneath waves. J. Fluid Mech. 147, 449-464.

Cheong, H.-F., Jothi Shankar, N. and Subbiah, K. (1989). Inertia dominated forces on submarine pipelines near seabed. J. of Hyd. Res. 27(1), 5-22.

Dean, W.R. (1948). On the reflection of surface waves by a submerged cylinder. Proc. Camb. Phil. Soc., 44, 483-491.

Dold, J.W. and Peregrine, D.H. (1984). Steep unsteady water waves. An efficient computational scheme. Proc. 19th ICCE, Houston, Texas, 1, 955-967. ASCE, New York, 1985.

Grilli, S.T., Skourup, J. and Svendsen, I.A. (1989). An efficient boundary element method for non-linear water waves. Engineering Analysis with Boundary Elements. 6(2), 97-107.

Isaacson, M. and Cheung, K.-F. (1990). Time-domain solution for second-order wave diffraction. J. of Waterway, Port, Coastal and Ocean Engineering, 116 (2), 191-210.

Longuet-Higgins, M.S. and Cokelet, E.D. (1976). The deformation of steep surface waves on water. I. A numerical method of computation. Proc. Roy. Soc. London, A 350, 1-26.

Milne-Thomson, L.M. (1968). Theoretical Hydrodynamics. 4th ed. MacMillan, London.

Miyata, H. and Lee, Y.-G. (1990) Vortex motions about a horizontal cylinder in waves. Ocean Engineering, 17 (3), 279-305.

Ogilvie, T.F. (1963). First and second order forces on a cylinder submerged under a free surface. J. Fluid Mech., 16, 451-472.

Rienecker, M.M. and Fenton, J.D. (1981). A Fourier approximation method for steady water waves. J. Fluid Mech., 104, 119-137.

Skourup, J. (1989). A boundary integral equation model for the development of non-linear water waves and their interaction with structures. Ph.D. dissertation. Series Paper No. 47. xvi + 158 pp. Institute of Hydrodynamics and Hydraulic Engineering (ISVA). Technical University of Denmark.

Skourup, J. and Jonsson, I.G. (1990). Computations of forces and particle orbits around horizontal cylinders under steep waves. Submitted for publication.

Stansby, P.K. and Slaouti, A. (1984). On non-linear wave interaction with cylindrical bodies: A vortex sheet approach. Appl. Ocean Res., 6(2), 108-115.

Ursell, F. (1950). Surface waves in the presence of a submerged circular cylinder. Proc. Camb. Phil. Soc., 46, 141-158.

Vada, T. (1987). A numerical solution for the second-order wave diffraction problem for a submerged cylinder of arbitrary shape. J. Fluid Mech., 174, 23-37.